Research Article

Khaleeq Uz-Zaman, Jehan Bakht, Bates Kudaibergenova Malikovna, Eman R. Elsharkawy*, Anees Ahmed Khalil, Saud Bawazeer*, and Abdur Rauf*

Trillium govanianum Wall. Ex. Royle rhizomes extract-medicated silver nanoparticles and their antimicrobial activity

https://doi.org/10.1515/gps-2020-0054
received May 13, 2020; accepted August 09, 2020

Abstract: Synthesis of nanoparticles is a fast-growing area of interest in the current development in science and technology. Nanoparticles are also used in biomedical applications. Green synthesis of nanoparticles is an environmental friendly and cost-effective technique. *Trillium govanianum* Wall. Ex. Royle crude extract was used for the eco-friendly genesis of silver nanoparticles (AgNPs). Aromatic amines were the functional groups involved in the biofabrication and synthesis of the AgNPs. The production of AgNPs was established by the appearance of brown color. The manufactured AgNPs were characterized by UV-Vis spectrophotometer, X-ray diffractometer, and FTIR spectrophotometer. AgNPs were face-centered cubic in nature with an average size of 9.99 nm. The produced AgNPs (18 μL $disc^{-1}$) showed substantial antibacterial (53.74, 52.75, 51.61, 43.00, 36.84, and 36.84%) and antifungal (54.05, 42.11, 41.10, 40.85, 30.55, and 29.73%) potential against the tested bacterial (*X. campestris*, *P. aeruginosa*, *S. aureus*, *E. coli*, *B. subtilis*, and *K. pneumoniae*) and fungal (*A. alternaria*, *Paecilomyces*, *C. albicans*, *Curvularia*, *A. niger*, and *Rhizopus*) strains, respectively.

Keywords: *Trillium govanianum*, AgNPS, UV, FT-IR, X-ray diffractometer

1 Introduction

Nanotechnology deals with the production and synthesis of particles having a size in the range of 10–100 nm with unique properties depending on the size in health and energy. Various techniques are available for the synthesis of nanoparticles. Among these techniques, only green synthesis is eco-friendly, cost-effective, and energy-efficient [1]. Due to various environmental and production issues, the current study primarily focuses on the green synthesis of nanoparticles using silver nitrate [2–4]. Silver nanoparticles (AgNPs) have strong antimicrobial activities and can attack a broad range of targets in microorganisms, such as proteins with thiol groups, cell walls, and cell membranes. AgNPs show antimicrobial activities against various infectious organisms [5,6]. Depending upon their antimicrobial activity, AgNPs can play a promising role in the food packaging system to prevent the growth of fouling contaminants and to improve the shelf life of food. AgNPs are also used in drug delivery for various diseases. In treatments, AgNPs display cytoprotective activity against HIV-1 infected cells [7,8]. Numerous nanoparticles have been formulated using different physical, chemical, and green nanoparticle synthesis techniques. Among all of these, green synthesis methods are known to be the most economical and environmental friendly technique owing to the use of natural compounds in the development of nanoparticles [9]. Various studies have shown the use of different plant extracts for the formulation of AgNPs.

* **Corresponding author: Eman R. Elsharkawy,** Chemistry Department, Faculty of Science, Northern Border University, Saudi Arabia, e-mail: elsharqawyeman2017@gmail.com, mashaljcs@yahoo.com
* **Corresponding author: Saud Bawazeer,** Department of Pharmaceutical Chemistry, Faculty of Pharmacy, Umm Al-Qura University, Makkah, P.O. Box 42, Saudi Arabia, e-mail: ssbawazeer@uqu.edu.sa
* **Corresponding author: Abdur Rauf,** Department of Chemistry, University of Swabi, Swabi, Anbar, KPK, Pakistan
Khaleeq Uz-Zaman, Jehan Bakht: Institute of Biotechnology and Genetic Engineering, The University of Agriculture, Peshawar, KPK, Pakistan
Bates Kudaibergenova Malikovna: Department of Chemistry and Chemical Technology, Al-Farabi Kazakh National University, Almaty, Kazakhstan
Anees Ahmed Khalil: University Institute of Diet and Nutritional Sciences, Faculty of Allied Health Sciences, The University of Lahore, Pakistan

These synthesized AgNPs have been studied in various in vitro antimicrobial assays to validate their antibacterial and antifungal activities [10–13].

Trillium govanianum is a member of the family melanthiaceae that is distributed from Pakistan to Bhutan between the height that ranges from 2,500–400 m above the sea level crosswise the Himalayan region [14]. *T. govanianum* is a native species of the Himalayan region, habitually favoring shaded parts in the forest for its normal growth. It is a small herb having three leaves in one entire at the summit of the stem and possess solitary purple flowers in the center while leaves are generally ovate, clearly stalked, and actuate [14]. The rhizomes of *T. govanianum* comprise trillarin which on hydrolysis contains 2.5% diosgenin which is used for the preparation of steroidal as well as sex hormones [15]. The rhizomes are traditionally used for the treatment of menstrual and sexual disorders, dysentery, healing of wounds, inflammation, etc. [15]. Steroids, steroidal glycosides, and steroidal saponins have been isolated from different species of *Trillium* [16]. Keeping in view the medicinal applications of *Trillium govanianum*, the current study was designated to explore the green synthesis of AgNPs to examine its antimicrobial potential.

2 Materials and methods

The current research was conducted at IBGE, The University of Agriculture, Peshawar. *T. govaninum* rhizomes were collected from the high-altitude terrain of District Battagram, KPK Pakistan, and identified at the Department of the Botany University of Peshawar. The voucher specimen no. UOS (Bot432) was deposited in the herbarium of the above-mentioned department.

2.1 Extract preparation and synthesis of nano-particles

Extract preparation and green synthesis of silver nanoparticles and their characterization were carried out as described methods [14].

2.2 Antimicrobial activity

Antimicrobial activity of different microbes was determined by Bakht et al. [17] against *C. albicans*, *Curvularia*, *R. oryzae*, *A. niger*, *A. alternaria*, *Rhizopus*, *Paecilomyces*, *B. subtilis*, *P. aeruginosa*, *E. coli*, *K. pneumoniae*, *S. aureus*, and *X. campestris*.

3 Results and discussions

3.1 Effect of different reaction mixtures on the stability of prepared AgNPs

Green synthesis of the AgNPs and effective reduction of silver from Ag^{+} to Ag^{0} was confirmed by the change in color from colorless to brown in the combination mixture (Figure 1). The changed color of the solution when measured at different wavelength confirmed the production of silver nanoparticles [15]. The reaction mixture (1:1), in which reduction of Ag^{+} ions just occurred, with moderate surface plasma resonance (SPR), band intensities, and wide peak suggested partial reduction of Ag^{+} ions and formation of higher concentration of AgNPs with SPR at 430 nm. At reaction mixture (1:2), the observed intensity of SPR peak was more with small sharpness in the peak when compared with the reaction mixture of 1:1 with SPR at 430 nm. Furthermore, at reaction mixture (1:9), the SPR band intensity and peak were highest indicating a complete reduction of silver ions with SPR at 407.98 nm. Thus, the maximum yield of reduced size of AgNPs observed at reaction mixture (1:9) suggested optimum reaction conditions under room temperature (Figures 2 and 3). Further increase in the ratio of $AgNO_3$, there was the appearance of a blue shift which is the confirmation of destabilized synthesis and deformed nanoparticles. It may be assumed that it is the result of the saturation of the biomolecules' functional groups responsible for the synthesis of the nanoparticles

Figure 1: Digital optical images of synthesized silver nanoparticles color change of silver nitrate to silver nanoparticles.

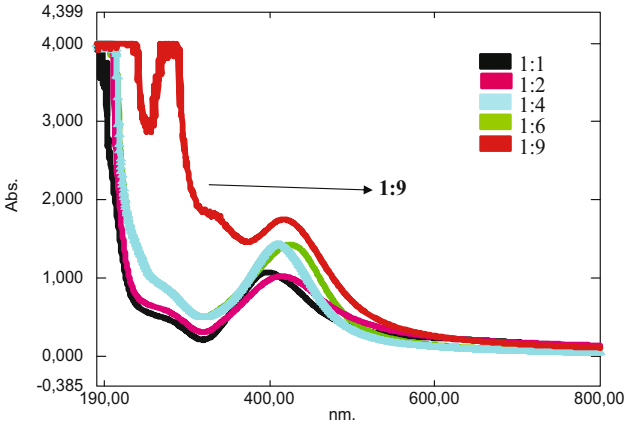

Figure 2: Optimization of silver NPs of pure extracts of *T. govanianum*.

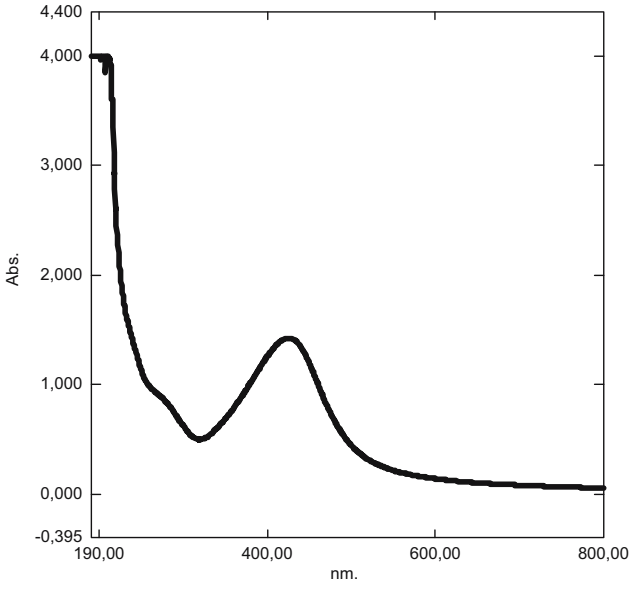

Figure 4: Bioinspired silver nanoparticles spectra prepared by utilizing 1 mL pure *T. govanianum* extract solution with 9 mL of silver salt (0.1 mM) solution. The sharpest peak of the silver nanoparticles (AgNPs) is at 407.98 nm.

with Au ions and less availability of the compounds [16,18]. The UV-Vis spectrum showed that the maximum absorption peak was recorded at the wavelength of 407.98 nm, which is corresponding to the silver nanoparticles absorption range that is 350–450 nm, showing the absorbance of 1.5 crude extract of *Trillium govanianum* (Figure 4).

To optimize the synthesis of the bioinspired eco-friendly AgNPs, they were evaluated for various kinds of stability tests, consisting of NaCl concentrations stress, temperature effect, and pH effect using UV-Vis spectrophotometer. These stresses exert a characteristic effect on the fabrication, stability, shape, size, and morphology of AgNPs. Bioinspired silver nanoparticles of the plant extracts indicated that thermal stress can adversely affect the production and reliability of the optimized nanoparticles (Figure 5).

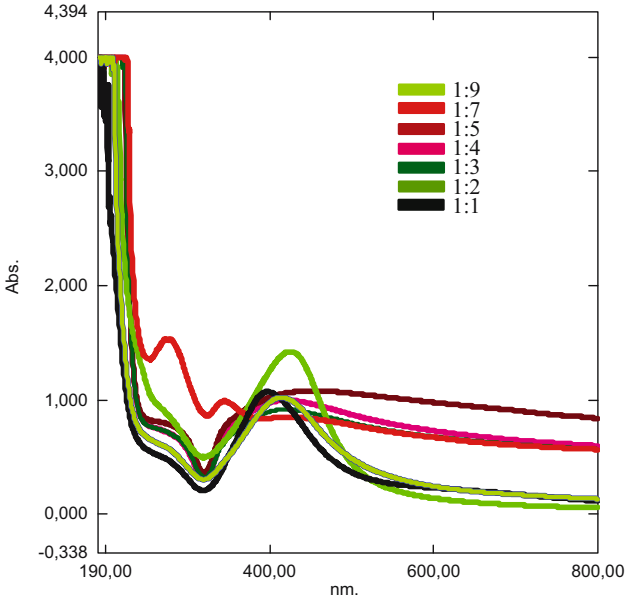

Figure 3: Evaluation of various bioinspired silver nanoparticles spectra prepared by utilizing 1 mL pure plant extract solution with different ratios of silver salt (0.1 mM) solution.

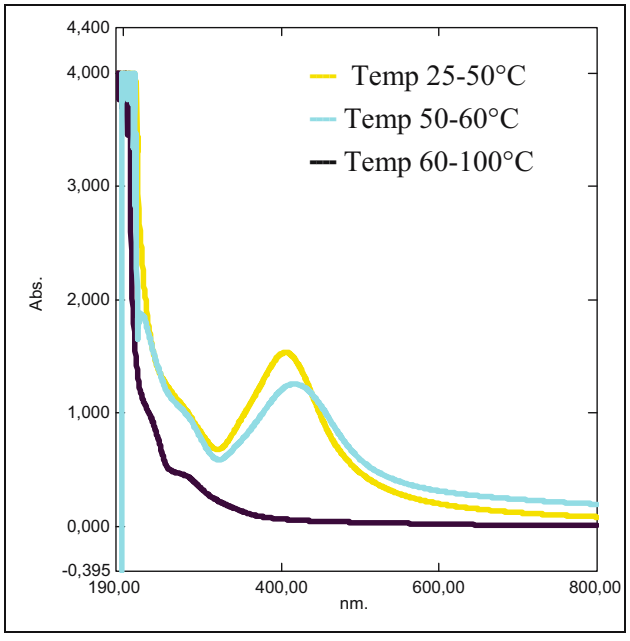

Figure 5: UV-spectra showing the effect of thermal stress on the deformation and synthesized of AgNPs of *T. govanianum*.

3.2 Effect of temperature on the stability of prepared AgNPs

Results revealed that AgNPs of plant extracts indicated a maximum thermal stability in the temperature range of room temperature to 50°C and a most intense and sharp peak was observed. Our results are in accordance with earlier findings of Ganesan et al. [19], who revealed that the synthesis of bioinspired AgNPs is optimal in the temperature range of 20°C to 50°C. The proliferation in temperature amplified the bands of the reaction combination which displayed superior production of AgNPs. Additionally, improved SPR bands were unveiled at this temperature with a slender absorption range demonstrating the severe discrepancy of the manufactured AgNPs. Data in the thermal range from 50°C to 60°C further indicated that heating adversely affect the thermal stability of the green synthesized silver nanoparticles as they were destabilized in this range. The sharpness of the peak in this high-temperature range is low as compared to the low-temperature range revealing the distortion and deterioration of the biological nanoparticles due to thermal stress. Further elevation in the temperature (from 60°C to 100°C) resulted in complete distortion and deterioration of biologically synthesized AgNPs as no peak was observed spectrophotometrically [20].

3.3 Effect of pH on stability of prepared AgNPs

The effect of pH on the consistency and formation of the environment-friendly manufacturing of the AgNPs is shown by the UV spectrophotometer profile. To study the pH effect, one normal sodium hydroxide (1 N NaOH) was used as basic stress while one normal hydrochloric acid (1 N HCl) was used as acidic stress. The spectrophotometric bands of the biologically synthesized AgNPs were assessed for the various levels of pH stresses ranging from pH 3 to 9 (Figure 6). The UV data specified that pH plays an important role in the production and stability of AgNPs by directing the figure, dimension, and crystallinity of the AgNPs [20]. Spectrophotometric data further revealed that the produced sustainable particles were highly stable in the neutral to basic pH because the maximum absorption was recorded by silver nanoparticles in the solution whose pH was modified to 7–8. UV data verified that at pH 3, macro size silver nanoparticles

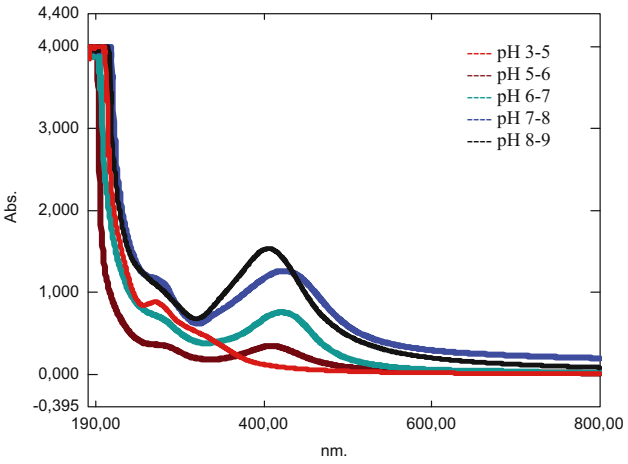

Figure 6: UV-spectra showing the effect of pH on the deformation of the synthesized AgNPs of *T. govanianum*.

were produced showing complete deterioration, while at higher alkaline/basic pH, more established and nano-size silver nanoparticles were formed. Outcomes of our present study were in harmony with the findings of Amit et al. [21]. Normally, the biogenic noble nanoparticles are supposed to be highly resistant in the basic pH range, as exhibited by the spectrophotometer pattern. The data on the other hand also revealed that green synthesized particles were less resistant to low pH (pH 3–6). The results also confirmed that at the lowest pH such as 3–5, there is complete deformation and deterioration of the majority of the produced nanoparticles as very weak and broad peaks were recorded by the UV-Vis spectrometer. Ashok et al. [22] analyzed various experiments and stated that biogenic silver nanoparticles are more resistant to deformation and deterioration in the alkaline pH [22]. It also appeared to regulate the character, dimension, and crystallinity of the AgNPs [23]. Earlier studies showed that pH had a considerable result on the size, shape, and hence on the reliability of the AgNPs [24]. Their results concluded that at lower pH, there is generally clumping of the synthesized nanoparticles that inversely affect the process of the nucleation process, while at high alkaline pH, chances of nucleation are high instead of clumps formation, which ultimately leads to the synthesis of more stable and appropriate size AgNPs. The UV spectroscopic pattern verified the blue stretch which is the indication of synthesis of smaller-sized Ag nanoparticles. At lower and higher pH, accumulation of AgNPs are more likely to happen which in turn prevent the process of nucleation; on the other hand, in the pH range 5–7, there is more chance of nucleation and no chances of clumping of AgNPs which leads to high intensity and sharp band in the UV profile [25].

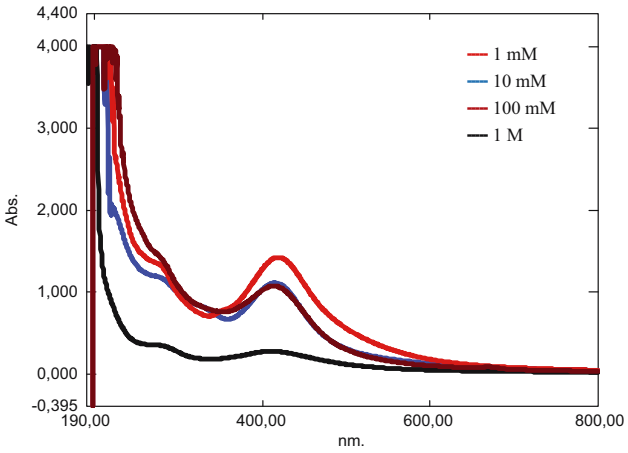

Figure 7: UV-Vis spectra showing the effect of NaCl stress on the deterioration and stability of the bioinspired silver NPs of *T. govanianum*.

3.4 Effect of different salt concentrations on the stability of prepared AgNPs

The stability test for the salt stress on the prepared and optimized AgNPs was performed using various concentrations of salt (NaCl). The results of the UV-Vis spectrophotometer indicated that increasing salt concentration also negatively affects the stability as well as the production of the nanoparticles (Figure 7). The data showed that salt concentration has an inverse relation with the stability of the synthesis of silver nanoparticles. Malarkodi et al. [26] also obtained similar results while performing salts stress on the optimized gold nanoparticles. The data further revealed that silver nanoparticles were highly stable at the lowest concentration that is in 1 mM, moderately stable at the 10 mM, weakly stable at 100 mM, and completely unstable at 1 M concentration of NaCl. The UV spectrum also indicated high saline stress as abrupt distortion and deformation of synthesized particles were noticed at a molar concentration as compared to milli molar concentration of salt. According to the UV pattern, 1 M salt stress have a maximum destabilizing effect on the synthesis of the green preparation of silver nanoparticles and cause deterioration of the AgNPs abruptly [27].

3.5 Atomic force microscopic (AFM) analysis

AFM measurement was led to reveal the size, shape, and 3D structure of the biodegradable Ag nanoparticles. AFM is a high-resolution microscopic technique that mainly focuses on the 3D structure of the particles under analysis. The microscopic data generated by AFM measurement validated that various sizes of recyclable

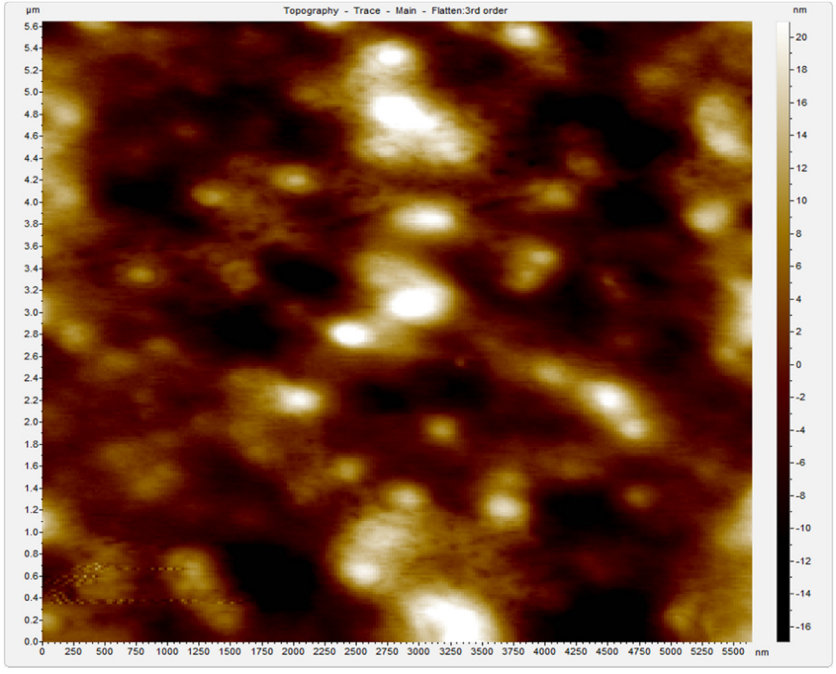

Figure 8: Showing circular and near-circular nanoparticles overlapping each other.

AgNPs were synthesized by a green approach. The approximate size of the smallest biogenic gold nanoparticle was found to be 6.5 nm while the size of the biggest AgNPs was calculated to be 65.5 nm. These AFM calculated results are exactly similar to the results of the X-ray diffraction (XRD) pattern analysis, where the size of crystallite was calculated to be 9.9 nm (Figures 8 and 9).

3.6 Scanning electron microscope (SEM) analysis

SEM analysis was carried out to establish the size and shape of the green-synthesized AgNPs (Figure 10). The image revealed that biologically prepared silver nanoparticles were distinctive and monodispersed. The scanning micrograph additionally indicated that the

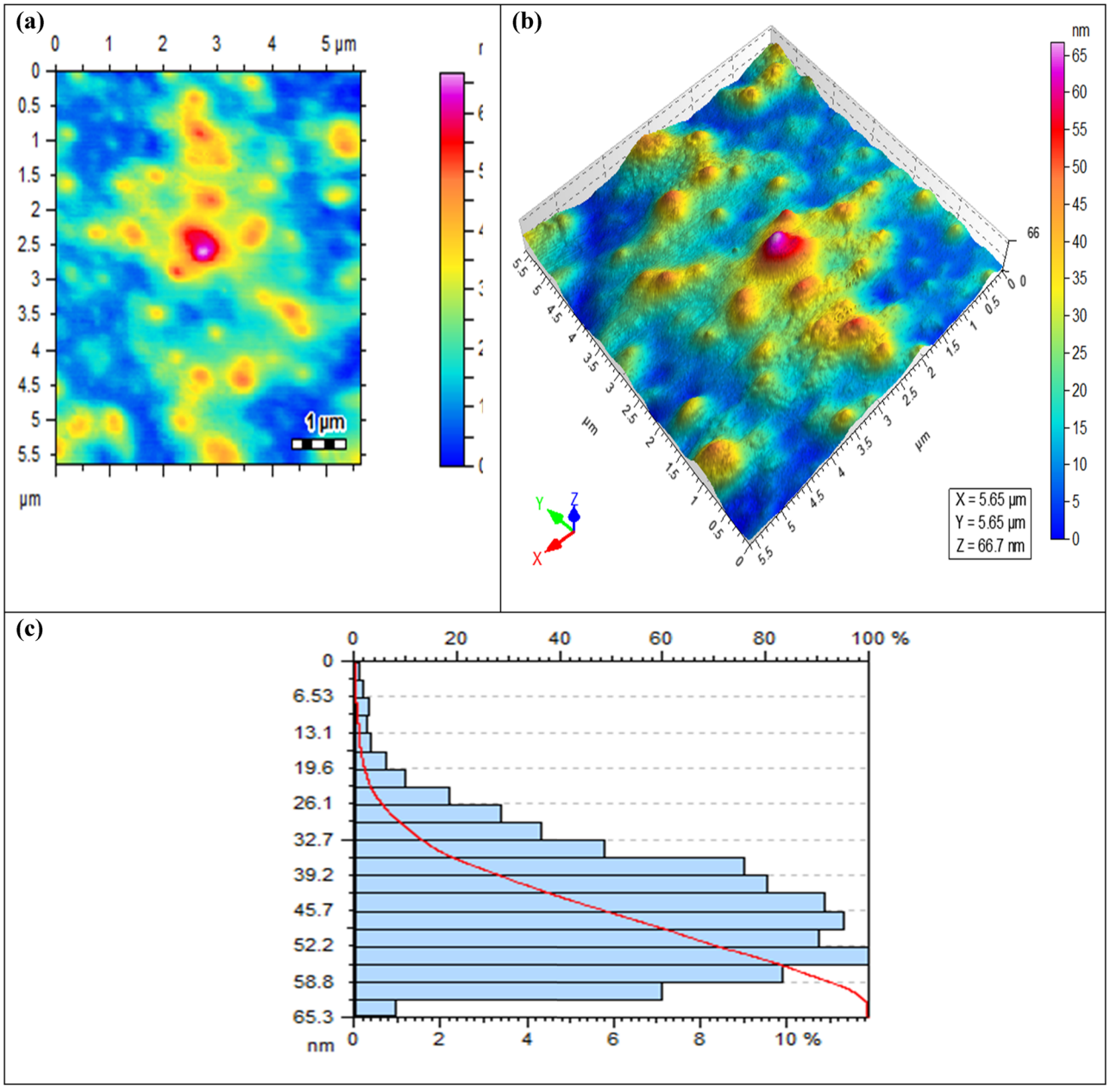

Figure 9: (a) Tapping mode AFM images of SNP synthesized with crude methanol fraction of *T. govanianum*. The scale bar of 100 nm is labeled in the image. (b) 3 µm × 3 µm AFM image showing a 2D view of silver NPs of *T. govanianum*. (c) Particle size distribution. The size distribution of synthesized SNP is shown.

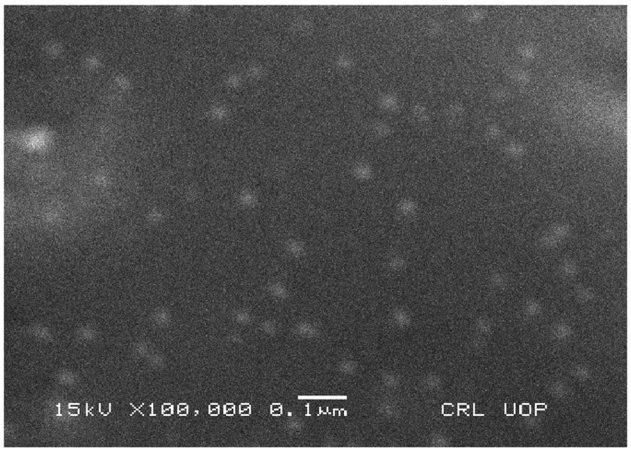

Figure 10: SEM image of the AgNPs after bio-reduction by *T. govanianum*.

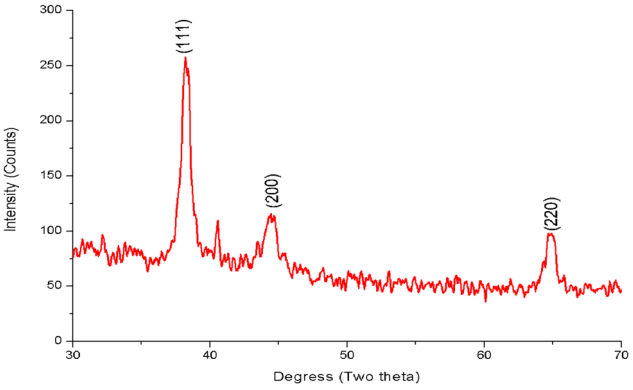

Figure 11: XRD patterns of silver NPs from *T. govanianum* showing the intense reflections with 2θ valves.

prepared particles were almost spherical in morphology. The diameter of the synthesized silver nanoparticles was calculated to be approximately 10 nm with uniform distribution. In the SEM analysis of the fabricated silver nanoparticles, none of them were found to be aggregated and was relatively easy to determine the monodispersed silver nanoparticles and calculate their approximate diameter in the nanometer range. To calculate the approximate size of the monodispersed AgNPs, scanning electron micrograph containing 100 particles was taken and the size was determined. The analysis revealed that these particles were in the range of 10–60 nm with an average size of 10 nm.

3.7 XRD analysis

AgNPs prepared by fabrication with plant extract were face-centered cubic (FCC) silver in nature as determined by XRD analysis (Figure 11). The XRD measurement indicated that in the 2θ range of 20°–80°, there were three sharp peaks at 37.50°(111), 44.13°(200), and 63.91°(220). These bands indicate that the crystallite is face-centered cubic in nature [28]. These results also clearly confirmed the high crystalline nature of AgNPs. The growth direction of the prepared crystallite was determined by the most intense bands at 37.50°, 111 as compared to the rest of the distinct bands. Sherrer's equation was employed to determine the average size of the obtained AgNPs from the extract. The approximate size of the nanoparticle was calculated based on a half-width full maximum of the most distinct peaks 111, 200, and 220 from the X-ray diffractogram. The approximate size of the crystallite was recorded as 9.99 nm based on Sherrer's equation [19]. The absence of any additional reflections except the reflections correspondent to the silver crystallite positively exhibited that bioinspired AgNPs were highly pure. While the weak reflections in the X-ray crystallography revealed the fixed nanocrystal in the dry freeze samples of the prepared nanoparticles. While calculating the typical size of the prepared NPs, the reflection of the most distinct peaks was utilized that are supposed to be 111, 200, and 220. The size of the nano-crystallite was revealed to be approximately 11 nm which was in close range to that of AFM size.

3.8 FT-IR analysis

Comparative analysis of the IR peaks of the biogenic nanoparticles and pure crude extract identified that absorption stretch at 1455.32 cm^{-1} in nanoparticles IR profile vanished completely which validate that the aromatic amines having –C–N functional are responsible for the stabilization and fabrication of nanoparticles (Figures 12 and 13). FTIR profile revealed that silver nanoparticles were synthesized by aromatic amines. Similarly on careful comparative analysis of the combined FT-IR profile of the plants' pure methanolic extract and prepared green nanoparticles additionally discovered a shift of approximately ±1 to 100 wavenumbers in the IR reflections. Peaks shifts were also observed in the broad spectrum range for pure AgNPs and plant extract as mentioned 3341.67–3340.34, 2925.77–2925.17, 1736.80–1740.76, 1634.95–1636.23, 1377.37–1377.98, 1046.01–1026.06 cm^{-1} [20,21]. The FTIR spectra of silver NPs reveals that peak at 3340 cm^{-1} might be attributed to the O–H bonds in OH-functional groups. C–H stretching of alkanes resulted in peaks at 2,925 cm^{-1}. Similarly, the

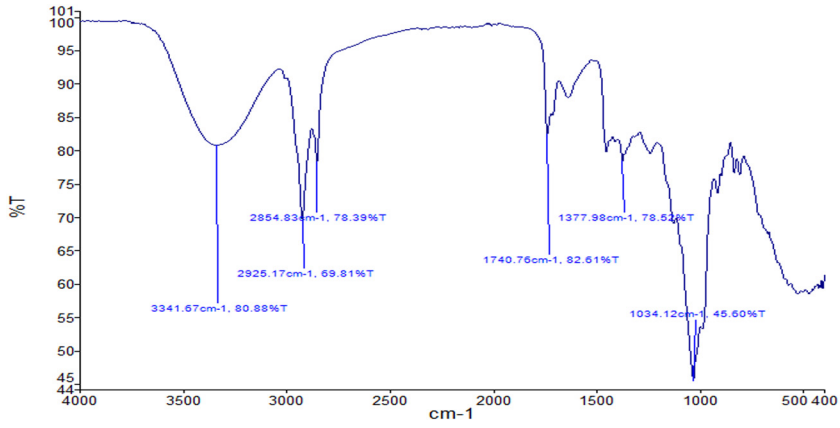

Figure 12: FTIR spectra of the crude methanol extract of *Trillium govanianum*.

peak noticed at 1,736 cm^{-1} might correspond to carbonyl groups. A distinct peak recorded in the region of 1,636 cm^{-1} may be related to C=O stretching frequency. An obvious peak at 1,377 cm^{-1} could be related to the stretching vibrations of alcohols, ethers, esters and carboxylic acids, and amino groups. One peak noticed in the region of 1,037 cm^{-1} might be attributed to N–C bond stretching of aliphatic amine groups. The results of our study are in agreement with previous studies on silver nanoparticles synthesized using different plant extracts [29].

3.9 Antimicrobial potentials of the prepared biogenic AgNPs using *T. govanianum* extracts

Similarly, the antimicrobial potentials of the biogenic AgNPs prepared by using plant extracts were also determined against various bacterial strains in the current study (Figure 14). Experimental results revealed that in the case of crude methanol AgNPs from the

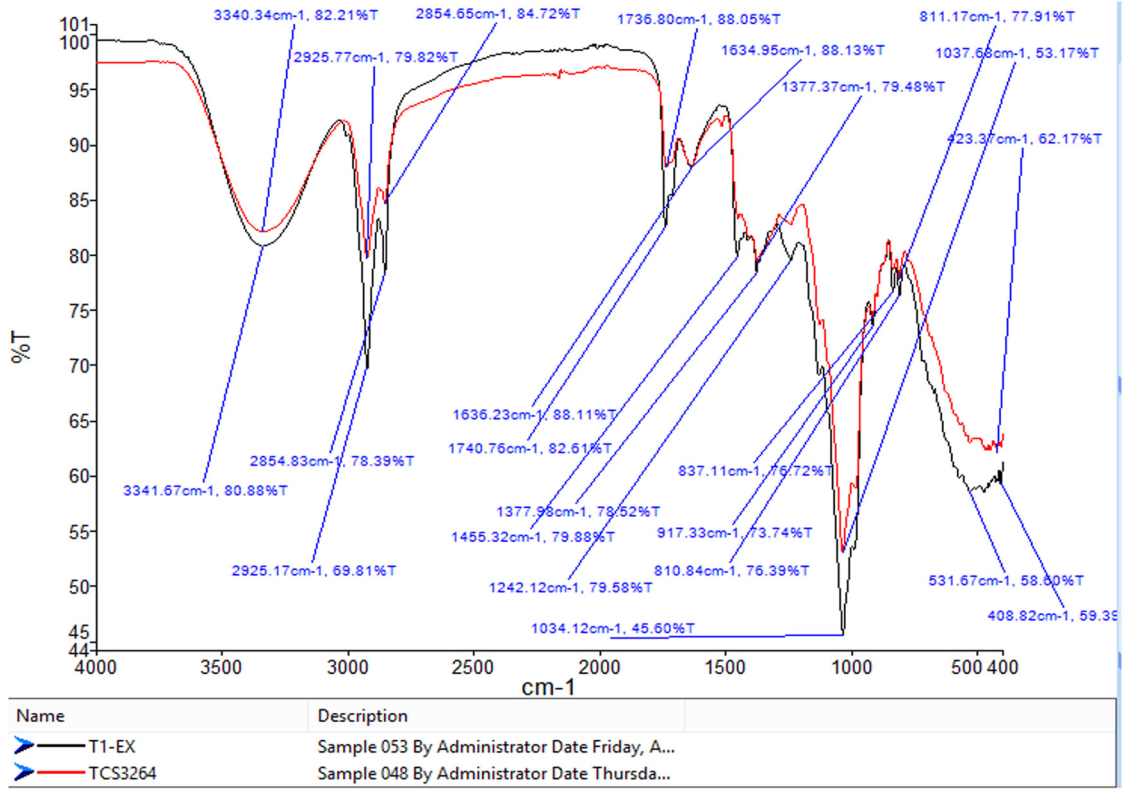

Figure 13: Comparative FTIR spectra of *T. govanianum* crude methanol extract and silver NPs

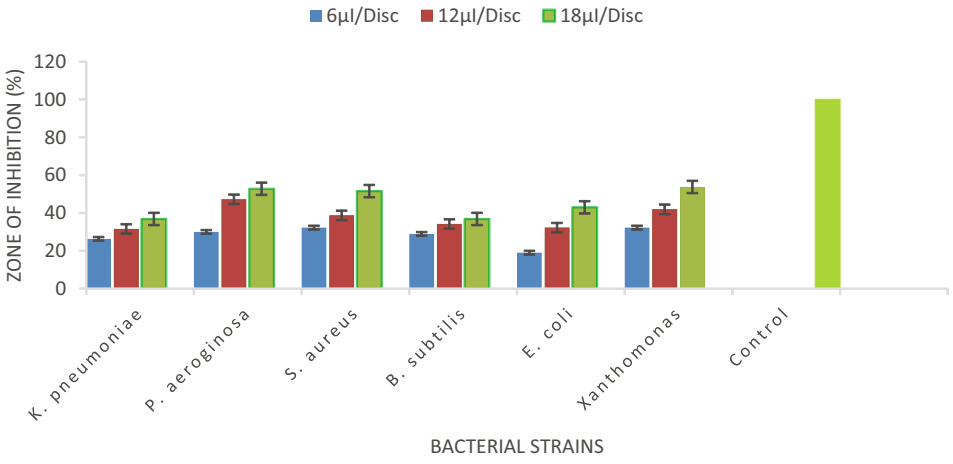

Figure 14: Antibacterial activity with a standard deviation of AgNPs of crude methanolic extract of *T. govanianum* against different bacterial strains by disc diffusion assay.

rhizome, the active zone of inhibition was observed by AgNPs at 18 µL disc^{-1} against *X. campestris* (53.74%) while the less effective zone of inhibition was confirmed at 6 µL disc^{-1} against *E. coli* (19.00%). Results also suggested that *X. campestris*, *P. aeruginosa*, and *S. aureus* displayed a maximum response to AgNPs, *B. subtilis* and *K. pneumoniae* displayed reasonable response while *E. coli* exhibited the least sensitiveness to AgNPs [30–32]. It was also concluded in the present work that the zone of inhibition depends on the dose of the bioinspired AgNPs. Bacterial strains display maximum growth retardation and inhibition to a high concentration of nanoparticles. Our results are in complete harmony with the conclusions of already documented literature [33,34]. Similarly, the antifungal activity of AgNPs of *T. govanianum* and against various fungal strains was carried out. It was identified that in the case of *T. govanianum*, crude methanol extract prepared AgNPs from the rhizome, maximum zone of inhibition was shown by AgNPs at 18 µL disc^{-1} against *A. alternaria* (56.76%) while *C. albicans* did not exhibit any response at all concentration and were resistant (Figure 15). It also revealed that no zone of inhibition was observed for any of the remaining tested strains at any applied concentration of the disc diffusion assay.

4 Conclusions

Green synthesis is an environment-friendly technique for the synthesis of nanoparticles. AgNPs were synthesized

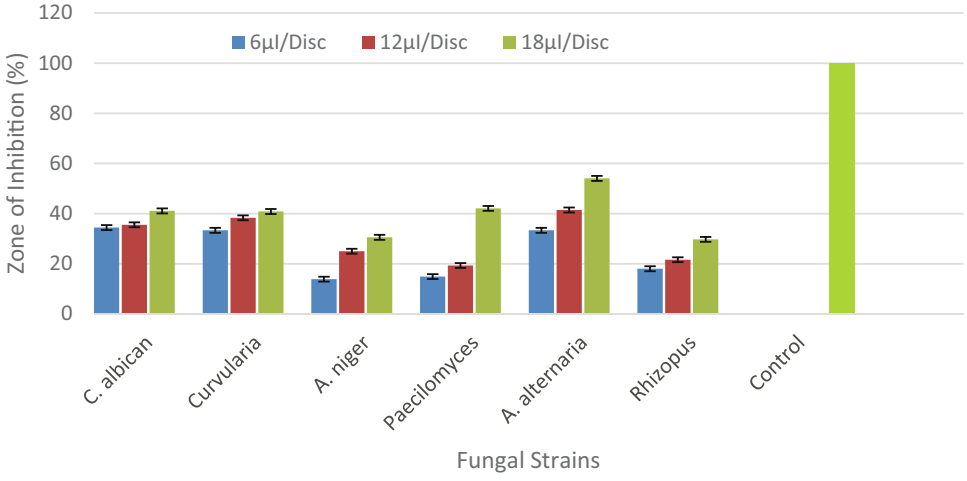

Figure 15: Antifungal activity with a standard deviation of AgNPs of pure ethanol extract of *T. govanianum* against different fungal strains.

in the present work using green technique and were characterized and verified by various methodologies. From the present work, we conclude that the synthesis of AgNPs using plant extract is an easy way, and nanoparticles are stable up to maximum temperature. Antibacterial and antifungal activities against various types were studied and give a good response. This study shows that these AgNPs have potential against bacterial and fungal infectious diseases.

Acknowledgments: The authors are grateful to the Higher Education Commission of Pakistan. This research was funded by the Higher Education Commission of Pakistan, NRPU/7343.

References

[1] Shedbalkar U, Singh R, Wadhwani S, Gaidhani S, Chopade BA. Microbial synthesis of gold nanoparticles: current status and future prospects. Adv Colloid Interface Sci. 2014;10:1016–25.
[2] Ravindran A, Chandran P, Khan SS. Biofunctionalized silver nanoparticles: advances and prospects. Colloid Surface B. 2013;105:342–52.
[3] Najeeb R, Khan A, Fatima U, Akram M, Al-musayieb N, Al-mussarani S, et al. Presence of Laxative and antidiarrheal activities in *Periploca aphylla*: a Saudi medicinal plant. Int J Pharmacol. 2013;10:1–7.
[4] Ateeq M, Shah MR, Ain N, Bano S, Anis I, Lubna, et al. Green synthesis and molecular recognition ability of patuletin coated gold nanoparticles. Biosens Bioelectron. 2015;63:499–505.
[5] Kim KJ, Sung WS, Suh BK, Moon SK, Choi JS, Kim JG, et al. Antifungal activity and mode of action of silver nano-particles on *Candida albicans*. Bio-metals. 2009;22:235–42.
[6] Narasimha G, Praveen B, Mallikarjuna K, Raju BDP. Mushrooms (*Agaricus bisporus*) mediated biosynthesis of silver nanoparticles, characterization and their antimicrobial activity. Int J Nano-Dimen. 2011;2:29–36.
[7] Sharma VK, Yngard RA, Lin Y. Silver nanoparticles: green synthesis and their antimicrobial activities. Adv Colloid Interface Sci. 2009;145:83–96.
[8] Kannan N, Subbalaxmi S. Biogenesis of nanoparticles a current perspective. Rev Adv Mater Sci. 2011;27:99–114.
[9] Fardsadegh B, Jafarizadeh-Malmiri H. Aloe vera leaf extract mediated green synthesis of selenium nanoparticles and assessment of their in vitro antimicrobial activity against spoilage fungi and pathogenic bacteria strains. Green Proc Synth. 2019;28:399–407.
[10] Chartarrayawadee W, Charoensin P, Saenma J, Rin T, Khamai P, Nasomjai P, et al. Green synthesis and stabilization of silver nanoparticles using Lysimachia foenum-graecum Hance extract and their antibacterial activity. Green Proc Synth. 2020;9:107–18.
[11] Anandalakshmi K, Venugobal J, Ramasamy V. Characterization of silver nanoparticles by green synthesis method using Pedalium murex leaf extract and their antibacterial activity. Appl Nanosci. 2016;6(3):399–408.
[12] Mražíková A, Velgosová O, Kavuličová J, Krum S, Malek J. The influence of silver nanoparticles synthesis on their properties. Acta Polytech. 2018;58:365–9.
[13] Ghanbari S, Vaghari H, Sayyar Z, Adibpour M, Jafarizadeh-Malmiri H. Autoclave-assisted green synthesis of silver nanoparticles using *A. fumigatus* mycelia extract and the evaluation of their physico-chemical properties and antibacterial activity. Green Proc Synth. 2018;7(3):217–24.
[14] Ullah F, Balht J, Shah S. Green synthesis and characterization of silver nano-particles from pharmaceutically important *Periploca hydaspidis* and their biological activity. Pak J Pharmaceut Sci. 2018;31:1267–77.
[15] Pantelis K, Delimitis A, Zaspalis V, Papadopoulos D, Sofia A, Michailidis TN. Green synthesis and characterization of silver nanoparticles produced using *Arbutus Unedo* leaf extract. Mat Lett. 2012;76:18–20.
[16] Amarendra DD, Gopal K. Biosynthesis of silver and gold nanoparticles using *Chenopodium album* leaf extracts. Colloids Surf A. 2010;369:27–33.
[17] Bakht J, Ali H, Khan MA, Khan A, Saeed M, Shafi M, et al. Antimicrobial activities of different solvents extracted samples of Linum usitatissimum by disc diffusion method. Afr J Biotechnol. 2011;10:19825–35.
[18] Umoren SA, Obot IB, Gasem ZM. Green synthesis and characterization of silver nanoparticles using red apple (*Malus domestica*) fruit extract at room temperature. J Mater Environ Sci. 2014;5:907–14.
[19] Ganesan V, Astalakshmi A, Nima P, Arunkumar C. Synthesis and characterization of silver nanoparticles using *Merremia tridentata* (L.) Hall. F. Int J Curr Sci. 2013;6:87–93.
[20] Bashir A, Ali J, Bashir S. Optimization and effects of different reaction conditions for the bioinspired synthesis of silver nanoparticles using *Hippophae rhamnoides* Linn. leaves aqueous extract. World Appl Sci J. 2013;22:836–43.
[21] Amit KM, Chisti Y, Banerjee UC. Synthesis of metallic nanoparticles using plant extracts. J Biotechnol Adv. 2013;31:346–56.
[22] Ashok B, Joshi B, Kumar AR, Zinjarde S. Banana peel extract mediated novel route for the synthesis of silver nanoparticles. Colloids Surf A. 2010;368:58–63.
[23] Raghavan V, Connolly JM, Fan HM, Dockery P, Wheatley A. Gold nanosensitisers for multimodal optical diagnostic imaging and therapy of Cancer. J Nanomed Nanotechnol. 2014;5:238–48.
[24] Huang J, Li Q, Sun D, Lu Y, Su Y, Yang X, et al. Biosynthesis ofsilver and gold nanoparticles by novel sundried Cinnamomumcamphora leaf. Nanotechnology. 2007;18:1–11.
[25] Krishnaraj C, Ramachandran R, Mohan K, Kalaichelvan PT. Optimization for rapid synthesis of silver nanoparticles and its effect on phytopathogenic fungi. Spectrochim Acta Part A. 2012;93:95–9.
[26] Malarkodi C, Rajeshkumar S, Vanaja M, Paulkumar K, Gnanajobitha G, Annadurai G. Eco-friendly synthesis and

characterization of gold nanoparticles using Klebsiella pneumoniae. J Nanostruct Chem. 2013;3:30–7.
[27] Noruzi M, Zare D, Khoshnevisan K, Davoodi D. Rapid green synthesis of gold nanoparticles using *Rosa hybrida* petal extract at room temperature. Spectrochim Acta Part A. 2011;79:1461–5.
[28] Linga RM, Savithramma N. Biological synthesis of silver nanoparticles using *Svensonia hyderobadensis*leaf extract and evaluation of their antimicrobial efficacy. J Pharmocol Sci Res. 2011;3:1117–21.
[29] Abbasi Z, Feizi S, Taghipour E, Ghadam P. Green synthesis of silver nanoparticles using aqueous extract of dried Juglans regia green husk and examination of its biological properties. Green Process Synth. 2017;26:477–85.
[30] Jayaseelan C, Ramkumar R, Rahuman A, Perumal P. Green synthesis of gold nanoparticles using seed aqueous extract of *Abelmoschus esculentus* and its antifungal activity. Ind Crops Prod. 2013;45:423–9.
[31] Mendez MAA, Martın-Martınez ES, Ortega-Arroyo L, Portillo GC, Espındola ES. Synthesis and characterization of silver nanoparticles: effect on phytopathogen *Colletotrichum gloesporioides*. J Nanopart Res. 2011;13:2525–32.
[32] Prasad TNVKV, Elumalai EK, Khateeja S. Evaluation of the antimicrobial efficacy of phytogenic silver nanoparticles. Asian Pacif J Trop Biomed. 2011;1:82–5.
[33] Sarvesh KS, Yamada R, Ogino C, Kondo A. Biogenic synthesis and characterization of gold nanoparticles by *Escherichia coli* K12 and its heterogeneous catalysis in degradation of 4-nitrophenol. Nano scale Res Lett. 2013;8:70–9.
[34] Logeswari P, Silambarasan S, Abraham J. Ecofriendly synthesis of silver nanoparticles from commercially available plant powders and their antibacterial properties. Sci Iranica. 2013;20:1049–54.

Appendix

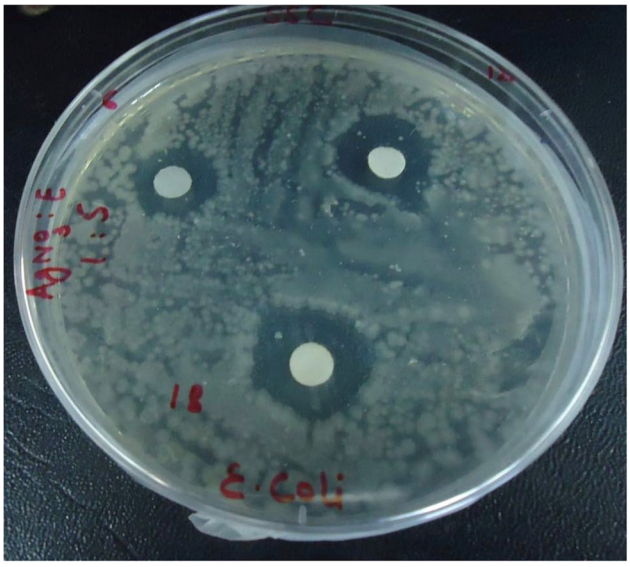

Figure A1: Antibacterial activity of AgNPs and crude methanolic extract of *T. govanianum* against *E. coli* by disc diffusion assay.

Figure A3: Antibacterial activity of AgNPs and crude methanolic extract of *T. govanianum* against *P. aeruginosa* by disc diffusion assay.

Figure A2: Antibacterial activity of AgNPs and crude methanolic extract of *T. govanianum* against *K. pneumoniae* by disc diffusion assay.